



ELSEVIER

Journal of Power Sources 93 (2001) 224–229

JOURNAL OF
**POWER
SOURCES**

www.elsevier.com/locate/jpowsour

Electrochemical characteristics of lithiated graphite (LiC_6) in PC based electrolytes

Hiroyuki Fujimoto*, Masahisa Fujimoto, Hiroaki Ikeda,
Ryuji Ohshita, Shin Fujitani, Ikuo Yonezu

New Materials Research Center, Sanyo Electric Co., Ltd., 1-18-13 Hashiridani, Hirakata, Osaka 573-8534, Japan

Received 3 April 2000; received in revised form 14 June 2000; accepted 1 September 2000

Abstract

The influence of the surface film formed on the graphite surface in ethylene carbonate (EC) on the lithium intercalation reaction into graphite in other electrolyte solutions including propylene carbonate (PC) was investigated. A graphite sample could be charged and discharged in PC + DME, while no lithium intercalation occurred in either PC + DMC or in PC + DEC. However, the lithiated graphite (LiC_6) obtained from a charge in EC with $1 \text{ mol dm}^{-3} \text{ LiPF}_6$ exhibited a reversible intercalation reaction with a large discharge capacity (370 mAh g^{-1}) and a good cycle performance even in PC + DMC. This result suggests that nature of the surface film formed in EC is a dominant factor in the reactivity of graphite with lithium ions in PC + DM, In PC + DME, the reversible capacity was smaller in both cases of the as-manufactured graphite and the LiC_6 obtained in EC. An XRD analysis indicated that the reduction in the crystalline size along the *c*-axis during the initial lithium intercalation is responsible for the smaller capacity. © 2001 Elsevier Science B.V. All rights reserved.

Keywords: Graphite; Surface film; Lithiated graphite; Lithium intercalation

1. Introduction

Graphite materials are now widely used as negative electrode materials for lithium ion batteries. As is well known, reactions of lithium intercalation into graphite materials are strongly affected by the electrolyte to be used, especially by the solvents therein [1–4]. For example, Dey and Sullivan have reported that the lithium ion intercalation into graphite in propylene carbonate (PC) is inert [1], whereas we have found that the electrolytes containing ethylene carbonate (EC) as a solvent enable the electrochemical synthesis of LiC_6 from graphite exhibiting a larger specific capacity and a better cycle performance [2]. In our previous work [5] we suggested that the surface film formed in EC enables the lithium ions to intercalate into the natural graphite. Therefore, the electrolytes containing EC are commonly used for lithium ion batteries with a graphite negative electrode material. However, we should also note that PC-based electrolytes are more desirable from the view point of the low-temperature performance of a lithium ion

battery, because the melting point of PC (-49°C) is much lower than that of EC (37°C).

In this paper, we investigated the electrochemical characteristics in PC-based electrolytes of the as-manufactured graphite and the LiC_6 obtained in EC in order to clarify the role of the surface film formed on the graphite surface in EC for the possible lithium ion intercalation in PC-based electrolytes.

2. Experimental

2.1. Preparation of the carbon electrode

Natural graphite (mean particle size: $20 \mu\text{m}$; specific surface area: $5 \text{ m}^2/\text{g}$; purity: above 99.9%) was used as an anode active material. The test electrode was fabricated by slurry-coating on a copper current collector sheet. The slurry was prepared by mixing the graphite powder and the polyvinylidene fluoride (PVdF) binder in the 1-methyl-2-pyrrolidone (NMP) solvent for a homogeneous mixture. The current collector sheet was then dried to evaporate NMP, and pressed to secure its conductivity and mechanical strength.

* Corresponding author. Fax: +81-72-841-0302.
E-mail address: h_fujimoto@rd.sanyo.co.jp (H. Fujimoto).

2.2. Preparation of the electrolyte

Three kinds of PC-based electrolytes containing $1 \text{ mol dm}^{-3} \text{ LiPF}_6$ were employed for electrochemical tests. The solvents for these electrolytes were prepared by mixing PC and a co-solvent of dimethyl carbonate (DMC), diethyl carbonate (DEC) or 1,2-dimethoxyethane (DME) (in the volumetric ratio of 1:1).

2.3. Electrochemical charge–discharge test

The electrochemical characteristics were measured using a three-electrode test cell with 40 ml of each PC-based electrolyte. Lithium metal was employed as a counter electrode and a reference electrode. The test cells were fabricated in an argon inert atmosphere, and then charged and discharged at a constant current density of 0.2 mA cm^{-2} between 0 and 1.0 V versus Li/Li^+ . For the lithiated graphite samples, the test was started from discharge (lithium de-intercalation).

2.4. Preparation of the lithiated graphite (LiC_6)

The lithiated graphite (LiC_6) was prepared by charging natural graphite in EC containing $1 \text{ mol dm}^{-3} \text{ LiPF}_6$. The chemical stability of the LiC_6 sample was checked by soaking it in each PC-based electrolyte (100 ml) for 5 days under an argon inert atmosphere. The electrochemical test in each PC-based electrolyte was done in the same manner as described above, while this test was started with a lithium de-intercalation. For both tests, the lithiated graphite sample was washed with excessive amount of each PC-based electrolyte (100 ml) before soaking or fabricating a test cell.

2.5. XRD analysis

The phase structure and crystallographic parameters of the samples were determined using powder X-ray diffractometry (XRD) with the $\text{Cu K}\alpha$ radiation passing through a graphite monochromator. The crystalline size along the c -axis (L_c) was determined from the full-width-at-half-maximum (FWHM) using the Scherrer equation as described in [6].

3. Results and discussion

3.1. Charge–discharge characteristics of the natural graphite in PC-based electrolytes

Fig. 1 shows the first charge and discharge curves of the sample graphite as manufactured in the three different PC-based electrolytes. For PC + DMC and PC + DEC, the electrode potential remained around 0.8 V versus Li/Li^+ , indicating that lithium intercalation did not occur. Previous studies [1,6] have shown that the electrolyte decomposition occurs at this potential level for these two electrolytes. On the other hand, for PC + DME, the sample could be charged and discharged. The first discharge capacity was 220 mAh g^{-1} , and the charge–discharge cycle efficiency in the first cycle was 52%. No capacity loss was observed during the first 10 cycles, as shown in Fig. 2.

3.2. Chemical stability of the LiC_6 sample

Fig. 3 shows photographs of the initial LiC_6 sample and the samples soaked in each electrolyte for 5 days. For PC + DMC and PC + DEC, the gold color attributed to

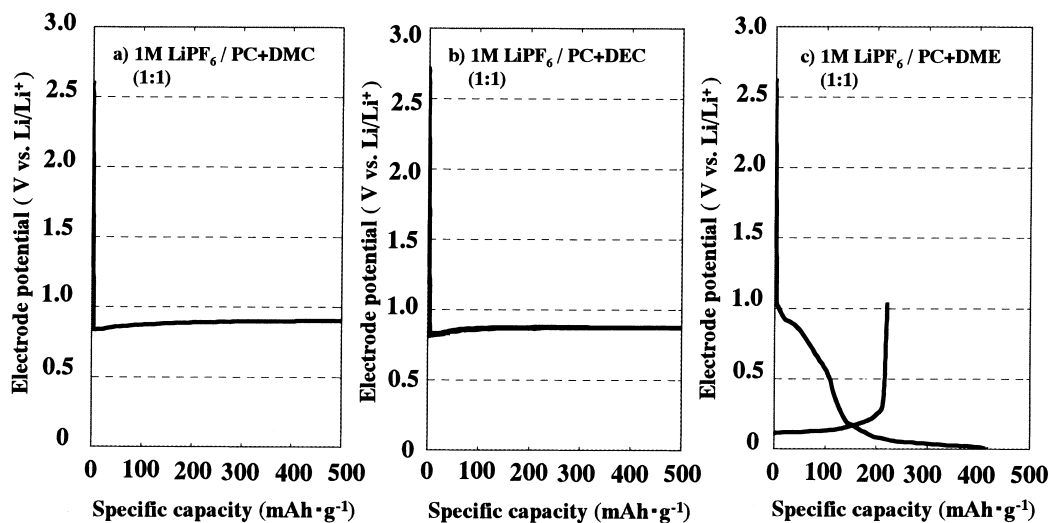


Fig. 1. Initial charge and discharge curves of the as-manufactured graphite in PC-based electrolytes: (a) $1 \text{ mol dm}^{-3} \text{ LiPF}_6/\text{PC} + \text{DMC}(1:1)$; (b) $1 \text{ mol dm}^{-3} \text{ LiPF}_6/\text{PC} + \text{DEC}(1:1)$; and (c) $1 \text{ mol dm}^{-3} \text{ LiPF}_6/\text{PC} + \text{DME}(1:1)$. Charge and discharge current density: 0.2 mA cm^{-1} , electrode potential range: 0–1.0 (V vs. Li/Li^+).

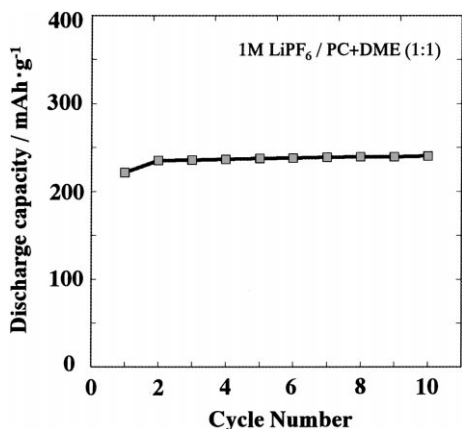


Fig. 2. Charge/discharge cycle characteristics of the as-manufactured graphite in $1 \text{ mol dm}^{-3} \text{ LiPF}_6/\text{PC} + \text{DME}(1:1)$. Charge and discharge current density: 0.2 mA cm^{-2} , electrode potential range: $0\text{--}1.0 \text{ (V vs. Li/Li}^+)$.

the LiC_6 phase remained unchanged, indicating that the stability of LiC_6 in these electrolytes was due to the protection provided by the surface film formed in EC from the reaction with the electrolyte. On the other hand, for PC + DME, the sample changed to dark brown. Fig. 4 shows the weakened LiC_6 peak and the strong LiC_{12} peak in the XRD pattern of the LiC_6 sample soaked in PC + DME for 5 days. These results indicate that the LiC_6 reacted with the electrolyte, and that the surface film formed in EC was not effective for the protection of the LiC_6 sample in PC + DME.

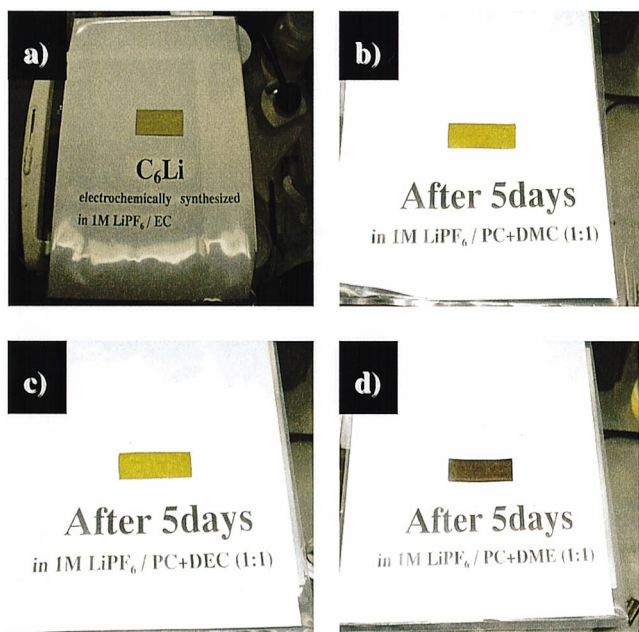


Fig. 3. Photographs of the LiC_6 samples synthesized in EC: (a) initial; (b) soaked in $1 \text{ mol dm}^{-3} \text{ LiPF}_6/\text{PC} + \text{DMC}(1:1)$ for 5 days; (c) soaked in $1 \text{ mol dm}^{-3} \text{ LiPF}_6/\text{PC} + \text{DEC}(1:1)$ for 5 days; and (d) soaked in $1 \text{ mol dm}^{-3} \text{ LiPF}_6/\text{PC} + \text{DME}(1:1)$ for 5 days.

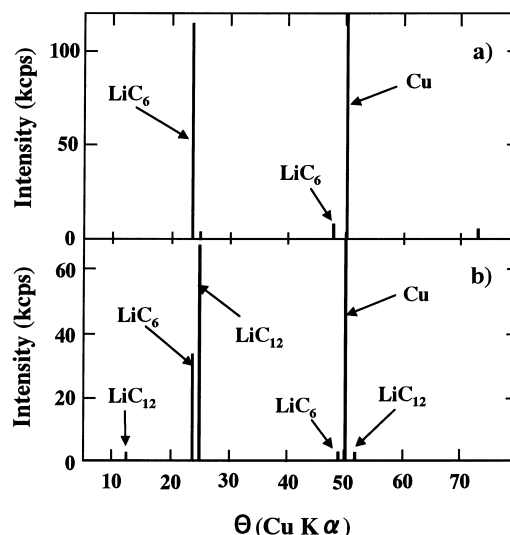


Fig. 4. XRD patterns of the LiC_6 samples: (a) before soaking (LiC_6), and (b) the sample soaked in $1 \text{ mol dm}^{-3} \text{ LiPF}_6/\text{PC} + \text{DME}(1:1)$ for 5 days.

3.3. Charge–discharge characteristics of the LiC_6 in PC-based electrolytes

Figs. 5–7 show the charge and discharge curves of the LiC_6 samples in PC + DMC, PC + DEC, and PC + DME, respectively. For DMC and DEC, the initial discharge capacity was approximately 370 mAh g^{-1} , which is close to the theoretical limit. For PC + DMC, no reduction of the discharge capacity was observed in the second cycle. However, for PC + DEC, the charge and discharge capacities drastically decreased, although the potential plateau corresponding to the electrolyte decomposition was not observed. Table 1 summarizes the comparison of crystal parameters between the LiC_6 sample prepared in EC and the sample after second charge in PC + DEC. The d-spacing parameters for the second charge in PC + DEC are similar to those in [7], and the d_{002} of LiC_6 is close to that before the electrochemical test. After the second charge PC + DEC, the L_c value slightly decreased in spite of the large decrease in the capacity. From these results, it is considered that the graphite structure did not change remarkably after the second charge in PC + DEC. It has been reported that the cycling efficiency of a lithium metal electrode is quite low in PC + DEC [8]. In our case, the color of the lithium counter electrode turned black after the first discharge, indicating that the passivation of the lithium counter electrode occurred during the first discharge. This observation and the XRD results suggests that the deterioration of the reversibility of the LiC_6 sample in PC + DEC is due to the passivation of the lithium counter electrode, not to the structural degradation of the sample. In the case of PC + DME, the first discharge capacity of 320 mAh g^{-1} was smaller than in the other cases. The sample was charged and discharged in the second cycle in the same way as in PC + DMC, but the discharge capacity

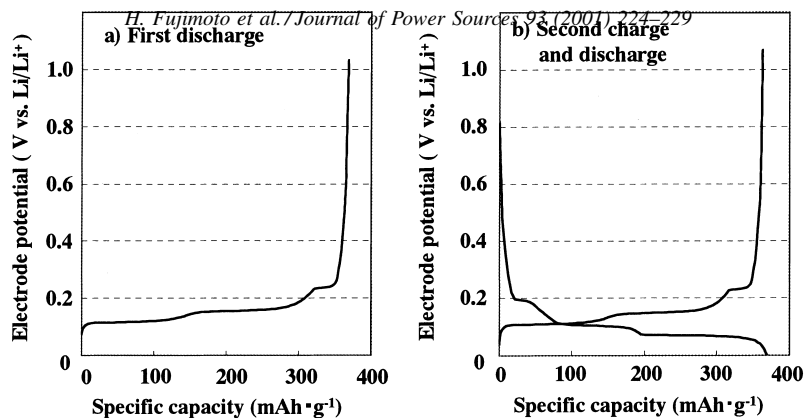


Fig. 5. Charge and discharge curves of the LiC_6 sample in $1 \text{ mol dm}^{-3} \text{ LiPF}_6/\text{PC} + \text{DMC}(1:1)$: (a) first discharge, and (b) second cycle. Charge and discharge current density: 0.2 mA cm^{-2} , electrode potential range: $0\text{--}1.0 \text{ (V vs. Li/Li}^+)$.

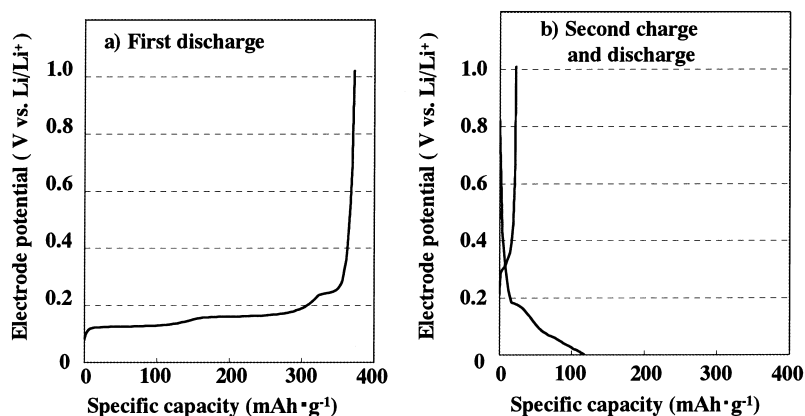


Fig. 6. Charge and discharge curves of the LiC_6 sample in $1 \text{ mol dm}^{-3} \text{ LiPF}_6/\text{PC} + \text{DEC}(1:1)$: (a) first discharge, and (b) second cycle. Charge and discharge current density: 0.2 mA cm^{-2} , electrode potential range: $0\text{--}1.0 \text{ (V vs. Li/Li}^+)$.

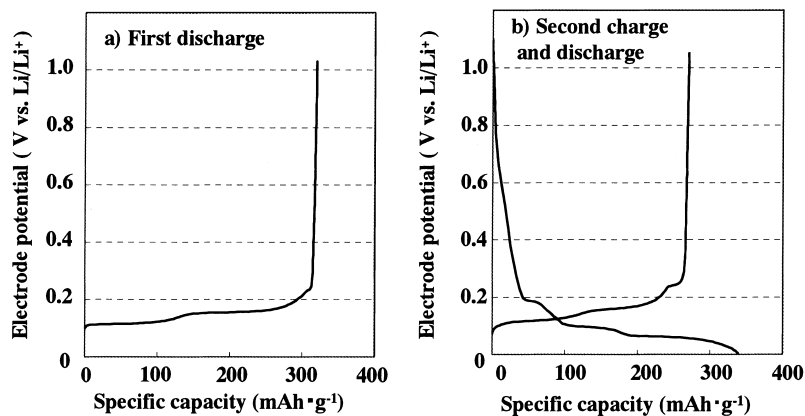


Fig. 7. Charge and discharge curves of the LiC_6 sample in $1 \text{ mol dm}^{-3} \text{ LiPF}_6/\text{PC} + \text{DME}(1:1)$: (a) first discharge, and (b) second cycle. Charge and discharge current density: 0.2 mA cm^{-2} , electrode potential range: $0\text{--}1.0 \text{ (V vs. Li/Li}^+)$.

Table 1

Crystal parameters of the lithiated graphite prepared in $1 \text{ mol dm}^{-3} \text{ LiPF}_6/\text{EC}$ and the sample after 2nd charge in $1 \text{ mol dm}^{-3} \text{ LiPF}_6/\text{PC} + \text{DEC}(1:1)$

Sample		$d \text{ (\AA)}$	Relative L_c value*
(a) Lithiated graphite prepared in EC	LiC_6	3.743 (d_{001})	100
(b) After 2nd charge in PC + DEC	LiC_6	3.735 (d_{001})	83.5
	LiC_{12}	3.551 (d_{002})	89.4

* Ratio to L_c size of lithiated graphite prepared in EC.

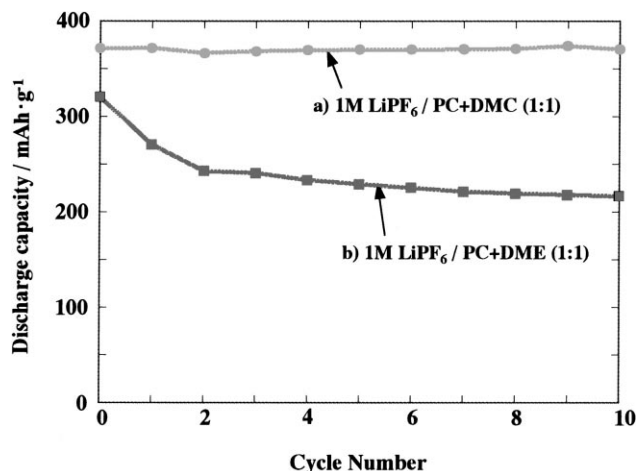


Fig. 8. Charge/discharge cycle characteristics of the LiC_6 obtained from charge in $1 \text{ mol dm}^{-3} \text{ LiPF}_6/\text{EC}$ in PC-based electrolytes: (a) $1 \text{ mol dm}^{-3} \text{ LiPF}_6/\text{PC} + \text{DMC}(1:1)$, and (b) $1 \text{ mol dm}^{-3} \text{ LiPF}_6/\text{PC} + \text{DME}(1:1)$. Charge and discharge current density: 0.2 mA cm^{-2} , electrode potential range: 0–1.0 (V vs. Li/Li^+).

decreased to 270 mAh g^{-1} . Fig. 8 shows the charge–discharge cycle characteristics of the LiC_6 sample in PC + DMC and PC + DME. For PC + DMC, the initial discharge capacity of 370 mAh g^{-1} was kept for the first 10 cycles. On the other hand, for PC + DME, the discharge capacity decreased during the initial stage, and then it was maintained around 220 mAh g^{-1} , which is close to the discharge capacity of the as-manufactured graphite in PC + DME.

3.4. Change in crystallographic parameters during charge and discharge

As the discharge capacity of carbonaceous materials is reported to correlate to their crystallinity [3,9,10], we investigated the change in the crystalline size along the c -axis (L_c) in order to explain the smaller reversible capacity in PC + DME. The change in L_c during the charge and discharge is summarized in Table 2. The crystalline size decreased drastically in the first lithium intercalation by

Table 2
Change in the crystalline size along the c -axis of the graphite samples during charge and discharge in $1 \text{ mol dm}^{-3} \text{ LiPF}_6/\text{PC} + \text{DME}(1:1)$

Sample	Crystalline size (ratio to the initial value, ^a in %)		
	After 1st charge	After 1st cycle	After 10th cycle
(a) Natural graphite as manufactured	39.9	40.7	32.4
(b) LiC_6 synthesized in EC	53.2	–	36.0

^a L_c size of natural graphite before charge/discharge cycle.

about 60% for the as-manufactured graphite and by 47% for the LiC_6 sample synthesized in EC. The crystalline size in both cases decreased to <40% of the initial value after the first 10 cycles. This size reduction is thought to be responsible for the smaller discharge capacity in PC + DME. For DME, both of chemical and electrochemical co-intercalation of solvent with lithium ion was studied [11–13]. Besenhard et al. reported the co-intercalation of solvent with lithium ion into HOPG in EC + DME, and proposed that this co-intercalation leads to the decomposition of the electrolyte and the HOPG structure, which brings the formation of the surface film [12]. Their model and our present results suggest that the electrochemical co-intercalation of DME occurring at the edge planes causes the destruction of the graphite crystal structure in PC + DME and the following formation of the suitable surface film for PC + DME system.

4. Conclusions

The influence of the surface film formed on the graphite surface in ethylene carbonate (EC) on the lithium intercalation reaction into graphite was investigated by testing LiC_6 samples synthesized in EC in various PC-based electrolytes. The conclusions are as follows:

1. The nature of the surface film formed in EC is a dominant factor in the reactivity of the graphite with lithium ions in PC + DMC. The LiC_6 prepared in EC can be charged and discharged with a large discharge capacity (370 mAh g^{-1}) and a good cycle performance even in PC + DMC.
2. In PC + DME, both the as-manufactured graphite and the LiC_6 sample can be charged and discharged with a moderate discharge capacity ($220\text{--}240 \text{ mAh g}^{-1}$) and a good cycle performance.
3. The smaller reversible capacity for PC + DME is due to the change in the crystalline size during a charge and discharge.

References

- [1] A.N. Dey, B.P. Sullivan, J. Electrochem. Soc. 117 (1970) 222.
- [2] M. Fujimoto, K. Ueno, T. Nohma, M. Takahashi, K. Nishio, T. Saito, in: Proceedings of the Symposium on New Sealed Rechargeable Batteries and Supercapacitors, 1993, p. 280.
- [3] K. Tatsumi, N. Iwashita, H. Sakaebe, H. Shioyama, S. Higuchi, A. Mabuchi, H. Fujimoto, J. Electrochem. Soc. 142 (1995) 716.
- [4] Y. Ein-Eli, S.F. Mcdevitt, R. Laura, J. Electrochem. Soc. 145 (1998) L1.
- [5] M. Fujimoto, Y. Shoji, Y. Kida, R. Ohshita, T. Nohma, K. Nishio, J. Power Sources 72 (1998) 226.
- [6] M. Fujimoto, Y. Kida, T. Nohma, M. Takahashi, K. Nishio, T. Saito, J. Power Sources 63 (1996) 127.
- [7] T. Ohzuku, Y. Iwakoshi, K. Sawai, J. Electrochem. Soc. 140 (1993) 2490.

- [8] K. Hayashi, S. Tobishima, J. Yamaki, in: Proceedings of the '95 Asian Conference on Electrochemistry, Osaka, Japan, May 1995, Extended Abstracts 3A-6, p. 140.
- [9] M. Takahashi, T. Nohma, M. Fujimoto, K. Nishio, T. Saito, in: Proceedings of the 33rd Battery Symposium, Tokyo, Japan, September 1992, Extended Abstracts, p. 217.
- [10] M. Endo, Y. Nishimura, T. Takeuchi, M.S. Dresselhaus, *J. Phys. Chem. Solids* 57 (1996) 725.
- [11] D. Ginderow, R. Setton, *C.R. Acad. Sci. Ser. C270* (1970) 135.
- [12] J.O. Besenhard, M. Winter, J. Yang, W. Biberacher, *J. Power Sources* 54 (1995) 228.
- [13] R. Yazami, S. Genies, *DENKI KAGAKU* 66 (1998) 1293.